Molecular Crystals and Liquid Crystals
Publication details, including instructions for authors and subscription information:
http://www.tandfonline.com/loi/gmcl16

Dynamic Behavior of Water in Lyotropic Ternary Mixtures

G. Chidichimo [a], A. Golemme [a], G. A. Ranieri [a], M. Terenzi [a] & J. W. Doane [b]

[a] Dipartimento di Chimica, Universita della Calabria, Arcavacata di Rende(CS), 87030, Italy

[b] Liquid Crystal Institute, Kent State University, Kent, Ohio, 44242, USA

Version of record first published: 20 Apr 2011.

To cite this article: G. Chidichimo , A. Golemme , G. A. Ranieri , M. Terenzi & J. W. Doane (1986): Dynamic Behavior of Water in Lyotropic Ternary Mixtures, Molecular Crystals and Liquid Crystals, 132:3-4, 275-288

To link to this article: http://dx.doi.org/10.1080/00268948608079548

Mol. Cryst. Liq. Cryst., 1986, Vol. 132, pp. 275–288
0026-8941/86/1324–0275/$20.00/0

Printed in the United States of America

Dynamic Behavior of Water in Lyotropic Ternary Mixtures

G. CHIDICHIMO, A. GOLEMME, G. A. RANIERI and M. TERENZI

Dipartimento di Chimica, Universita della Calabria, 87030 Arcavacata di Rende (CS), Italy

and

J. W. DOANE

Liquid Crystal Institute, Kent State University, Kent, Ohio 44242, USA

(*Received April 15, 1985*)

The diffusion of water molecules in lyotropic mixtures of potassium palmitate/potassium laurate/water was investigated using pulsed-field gradient nuclear magnetic resonance (PFG-NMR). The self-diffusion constant of water as a function of temperature was measured in two samples having different compositions and found to be sensitive to the structures of the different mesophases. Deuterium nuclear magnetic resonance (D-NMR) experiments were also performed on a mixture containing D_2O, in a temperature range where a rectangular mesophase (R_{α}) coexists with a lamellar (L_{α}) mesophase. The diffusion data, combined with the D-NMR spectral profiles allowed for the study of the size of the mixed mesophase domains.

INTRODUCTION

It has been recently discovered that lyotropic mixtures obtained from potassium palmitate (KP), potassium laurate (KL) and water show a very rich polymorphism. Aside from the well known lyotropic systems characterized by lamellar and cylindrical aggregates,[1] another lyotropic mesophase having ribbon-like aggregates inserted on a rectangular lattice can appear in the phase diagram as has been found by both x-rays[2] and deuterium nuclear magnetic resonance (D-NMR)[3,4] investigations of KP/KL/water lyotropic mixtures.

We present a further investigation of the KP/KL/water system giv-

ing the results obtained by measuring the diffusion of water as a function of the temperature and analyzing some D_2O-NMR spectral profiles. Sensitivity of the self-diffusion coefficient of water to the structure of the mesophase was found by other investigators[5] in closely related lyotropic systems.

The study by PFG-NMR technique was used for diffusion measurements in the samples reported in Table I. Sample A was investigated earlier[2-4,6] and shows the following sequence of mesophases:

$$L_\beta + R_\alpha \xleftrightarrow{35°C} L_\beta + RB_\alpha \xleftrightarrow{42°C} L_\alpha$$

where the symbols R_α, RB_α, L_α, and L_β define lyotropic phases consisting of elongated cylindrical aggregates, elongated ribbon aggregates, lamellar bilayers with conformationally disordered chains, and lamellar bilayers with all trans chains, respectively.

Sample B has also been analyzed by D-NMR of selectively deuterated lipids.[7] It shows the following polymorphism:

$$L_\beta + R_\alpha \xleftrightarrow{36°C} RB_\alpha \xleftrightarrow{51°C} RB_\alpha + L_\alpha$$

Lyotropic mixtures C and D are two-component systems which were analyzed in order to obtain diffusion data from systems having a well known structure. In the temperature range of interest, samples C and D form L_α and H_α mesophases, respectively.

The first aim of the present work is further confirmation of the structure of the RB_α mesophase. The ribbon model for the RB_α mesophase is based mainly on the x-ray evidence of the existence of a rectangular spatial lattice and the presence of a strong asymmetry parameter in the D-NMR spectral profiles of water and lipid components.

TABLE I

Molar composition of the samples used for diffusion measurements

Sample	KP	KL	Water
A	12.33	1.67	86.00
B	7.92	1.11	90.97
C	12.5	--	87.5
D	3.9	--	96.1

Taking into account that this mesophase appears to be sandwiched in between lamellar mesophases or to coexist with them in the phase diagram, it is clear that the diffusion measurements of water as a function of the temperature and especially across the phase transitions represent valuable physical information for confirming the proposed model. The breaking of lamellar aggregates into elongated ribbons should correspond to the opening of new channels for water diffusion. The occurrence of phase transitions, where the RB_α mesophase is involved should then bring well defined variations in the slope of a logarithmic plot of the diffusion coefficient versus the inverse temperature.

A second point worth investigating is the spatial distribution of ribbon and lamellar aggregates where the RB_α and L_α mesophases coexist. Understanding this distribution could provide information on the physical mechanism through which the ribbon aggregates originate from the lamellae. It has been demonstrated in analyzing the D-NMR spectral profiles of selectively labelled lipid components that the concentration of KL and KP molecules is not homogeneous in the ribbon aggregates. More specifically, the shorter chain component appears to be greatly concentrated at the cylindrical edges of the ribbons where the surface curvature is greater.[7] It is possible to argue that the process of molecular segregation starts in the lamellar aggregates when the temperature is decreased below a certain value. The breakage of the lamellae into ribbons could be a consequence of this molecular segregation. If this is the case, a bulk sample in a two-mesophase region should look as it is schematically represented in Figure 1, that is to say, a dispersion of structurally different subdomains. Of course molecules could be exchanged between ribbon-like and lamellar aggregates existing in equilibrium at a given temperature. Nevertheless, exchange of lipid molecules seems to be very slow with respect to the NMR time scale, since spectra reported in previous works show quite sharp singularities.[3] This should not be the case for water molecules provided that the dimension of the subdomains shown in Figure 1 is shorter than the mean distance a molecule can diffuse in the characteristic time of the quadrupolar interaction. In order to study such an effect, D-NMR spectral profiles of D_2O, taken from sample B, above 51°C, have been analyzed.

Finally, by combining the information obtained by measuring the diffusion with the PFG technique and those derived by analyzing D_2O spectral profiles, it has been possible to estimate the typical size of the mesophase subdomains present in sample B in the temperature range between 72–78°C.

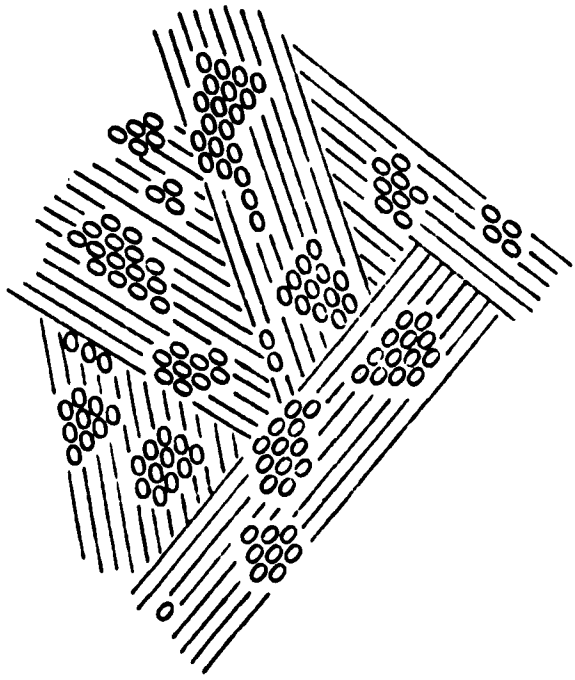

FIGURE 1 Illustration of a model for the spatial distribution of lyotropic aggregates in a two-phase region (L_α + RB_α) of a KP/KL/water ternary mixture.

EXPERIMENTAL

The samples described in Table I were prepared by weighing and mixing the components in a glass tube which was subsequently sealed under a nitrogen atmosphere. A very good homogenization of the samples was reached by alternatively heating and centrifuging the samples. Two mixtures corresponding to sample B were prepared: one containing protonic water for diffusion measurement and another containing D_2O for D-NMR investigation. It has been shown elsewhere[6,7] that, in the ternary mixtures considered, samples containing different deuterium labelled substances have the same phase transition temperatures when the molar percentages of the components remain constant.

These diffusion measurements were done by observing the H-NMR signal of the water at 35 MHz using a Polaron pulsed NMR spectrometer equipped with a sophisticated pulse programmer. A Datalab DL905 transient recorder, a Rockwell AIM 65 microcomputer and

a laboratory-constructed magnetic pulsed field gradient supply. The field gradient coil was wound in a Helmholtz pair configuration and was capable of supplying a field gradient up to 100 Gauss/cm.

The experiments were done by following the well known PFG procedure.[8] A magnetic field gradient pulse (MFGP) of duration δ was applied following a 90_x RF pulse, between the nuclear induction decay signal and the 180_y RF pulse. At a time Δ after the first gradient pulse, a second identical MFGP was applied between the 180_y RF pulse and the spin-echo. The signal was averaged on ten scans at a repetition rate of 15 seconds.

Deuterium NMR spectra were obtained by a Brucker WM300 spectrometer equipped with a broadband probe for deuterium. The quadrupolar echo technique was used to prevent loss of signal from the dead time of the receiver. The CYCLOPS[9] sequence was applied to eliminate line distortions from imperfect pulse length. A total of 500 scans was necessary to have an optimum signal-to-noise ratio. Spectra were taken by increasing the temperature to avoid super-cooling phenomena. A half-hour interval between spectra was used for temperature equilibration in both the PFG and D-NMR experiments. Tests for experimental repetivity were carried out.

RESULTS AND DISCUSSION

PFG experiments

Diffusion data were obtained by using the relation:

$$\ell n \frac{A^*(2\tau)}{A^\circ(2\tau)} = -\gamma g^2 D^2 \left(\Delta - \frac{1}{3}\delta\right) \qquad (1)$$

where A^*/A° is the attenuation factor due to spin diffusion, g the magnitude of the magnetic field gradient, D the translational diffusion coefficient, and γ the gyromagnetic ratio for the observed spin; δ and Δ, as stated earlier, are the width of the MFGP pulses and the time interval between MFGP pulses, respectively; τ is the separation between RF pulses. For the condition $\delta << \Delta$, D was obtained by plotting $\ell n\, A^*/A^\circ$ against Δ (in our experiments: $\delta = 7 \times 10^{-4}$ sec, $\tau = 10^{-2}$ sec and 4×10^{-3} sec $\leq \Delta \leq 1.6\ 10^{-2}$ sec). No evidence for restricted diffusion was found.

Results from sample A are shown in Figure 2 along with data obtained from the pure L_α mesophase of sample C, existing above

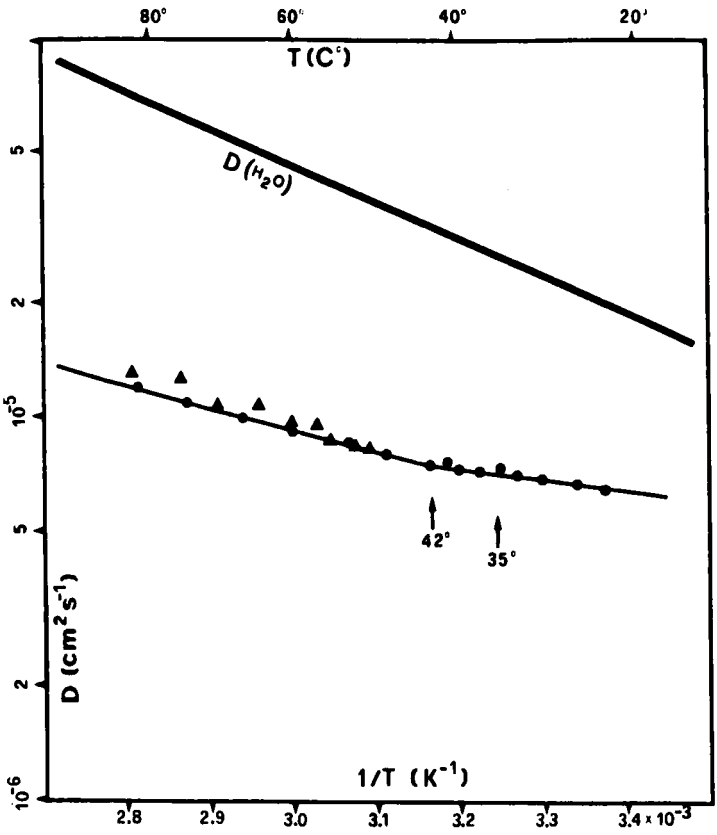

FIGURE 2 Temperature dependence of the diffusion constant obtained from the lyotropic mixtures:
● KP 12.33 m%, KL 1.67 m%, water 86.00 m% (sample A)
▲ KP 12.5 m%, water 87.5 m% (sample C)
Arrows at 42 and 35°C mark transitions $L_\alpha \rightarrow L_\beta + RB_\alpha$ and $L_\beta + RB_\alpha \rightarrow L_\beta + R_\alpha$, respectively.

50°C. Above 50°C the water diffusion coefficient is almost the same for both systems, indicating that in both the mixtures lamellar aggregates having the same extension and the same amount of defects do exist. The slope of $\ell n(D)$ versus 1/T has an appreciable variation at 42°C where previously reported D-NMR data[3] indicate the transition $L_\alpha \rightarrow L_\beta + RB_\alpha$. It must be noted that diffusion values below 42°C are higher than those corresponding to the extrapolation of the upper part of the plot. This is consistent with the gradual appearance of lyotropic aggregates of more reduced dimension resulting in an increase in the number of channels available to water diffusion. As

could be expected, the further transformation of the RB_α mesophase into the R_α mesophase does not introduce any further variation in the slope of the plotted data. In fact, the evolution of the ribbons into cylindrical aggregates cannot introduce dramatic variations in the water dynamics. This first experiment shows that the diffusion coefficient of the water is sensitive to the structure of the lyotropic aggregates even if it does not furnish any valuable information on the nature of the aggregates involved.

The strong dependence of the water mobility on the type of ag-

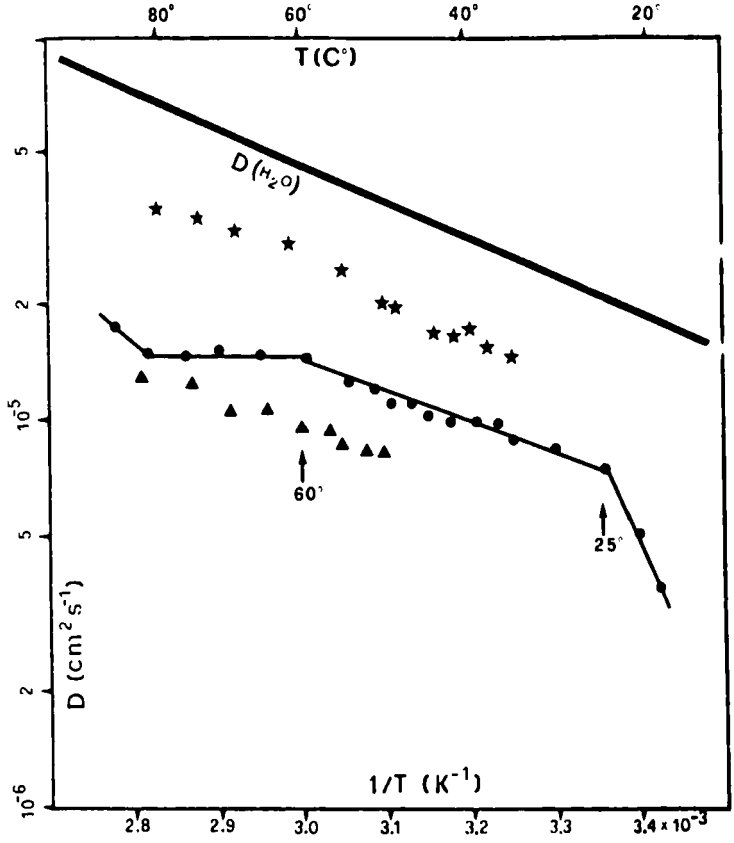

FIGURE 3 Temperature dependence of the diffusion constant obtained from the lyotropic mixtures:
● KP 7.92 m%, KL 1.11 m%, water 90.97 m% (sample B)
▲ KP 12.5 m%, water 87.5 m% (sample C)
★ KP 3.9 m%, water 96.1 m% (sample D)

gregates is better illustrated in Figure 3 where the result obtained from sample B, compared with the diffusion data relative to an L_α mesophase (sample C) and to an H_α mesophase (sample D), are shown. The experimental data obtained from sample B show very clearly the sequence of mesophases occurring when the temperature is changed. The diffusion increases very rapidly when the temperature is raised to 25°C. This confirms the interpretation that the system is in the two-phase regions, $L_\beta + R_\alpha$. The rapid increase of diffusion is due to the increase of the R_α mesophase with respect to L_β. Obviously the diffusion data do not give information on the precise shape of the aggregates but they indicate that one of the mesophases must be more fractured than any lamellar mesophase. The slope of $\ell n(D)$ against 1/T becomes much less steep between 25°C and 60°C. The D-NMR spectra of D_2O show two transitions centered at 36°C ($L_\beta + R_\alpha \rightarrow RB_\alpha$) and 51°C ($RB_\alpha \rightarrow RB_\alpha + L_\alpha$). No evidence of these transitions can be found in the diffusion data since the slope of $\ell n(D)$ versus 1/T seems almost continuous in the range 26–60°C. A simple explanation of this apparent discrepancy can be obtained by considering that D-NMR spectra of the water show that between 25°C and 36°C, as well as between 51°C and 60°C, the amount of the coexisting lamellar mesophases is a very small percentage of the dominant R_α and RB_α mesophases and consequently too small to affect water diffusion. The decrease in the slope at 25°C indicates that the transformation from the lamellar aggregates into the aggregates of more reduced dimension is almost over at 25°C and that no other quantitatively relevant phenomena occur below 60°C. The further decrease of the slope above 60°C is due to the gradual formation of the L_α mesophase and as a consequence of a gradual reduction in the number of diffusive channels. It is important to observe that the diffusion plot for the ternary mixtures remains sandwiched between those relative to the L_α and H_α mesophases given by the KP/water binary system. We believe that this is due to the fact that the dominant factor controlling the diffusion coefficient of the water is the percentage of water contained in the system. A greater content of water causes an increase in the diffusion coefficient probably because the amount of free water present in the sample increases also. A secondary but very important effect is the dependence of the diffusion on the structure. The interpretation of the data obtained on sample B can be perfectly rationalized in terms of the proposed structural models for the different mesophases which occur when changing the temperature. Experiments in progress seek a more quantitative explanation of the water diffusion in these lyotropic systems.[10]

Exchange of water from D-NMR spectral profiles

As indicated in the introduction, insight concerning the spatial distribution of ribbons and lamellar aggregates can in principle be obtained by analyzing the powder patterns of D_2O. It is obvious that if chemical exchange exists in the presence of the two coexisting mesophases, it should best be observed when the two mesophases have comparable populations. This condition is fulfilled in sample B in the temperature range between 72 and 78°C. The spectral profiles obtained in such conditions are shown in Figure 4. The central peak can be interpreted as the top part of a biaxial pattern analogous to that obtained from a RB_α mesophase,[3] while the symmetric external peak consists of 90° singularities coming from a uniaxial powder such as that obtained from L_α mesophases. It must be noted that the 0° shoulders are almost absent and that even the 90° singularities are quite smooth. A fitting of such patterns proved to be impossible even when considering a strong and not justified dipolar or quadrupolar relaxation broadening. In order to take into account these particular features of the D_2O spectral profiles a phenomena of chemical exchange of the water molecules among the two coexisting mesophases can be assumed. To verify this assumption the fitting of spectral profiles shown in Figure 4 was done by using the chemical exchange method proposed by Abragam.[11]

Before discussing the details of the line shape fitting, let us review some concepts concerning D-NMR spectroscopy. NMR spectra of deuterium nuclei are dominated by the quadrupolar interaction. In a liquid crystal sample this interaction gives rise to two spectral lines for each equivalent nuclear spin present in the observed molecule. The frequency of these lines with respect to the Zeeman frequency can be written as:[12]

$$\nu^{\pm} = \frac{3}{4}\nu_Q^{L.C.}\left\{\frac{3\cos^2\theta_o - 1}{2} + \frac{1}{2}\eta^{L.C.}\sin^2\theta_o\cos 2\phi_o\right\} \qquad (2)$$

Eq. (2) is particularly useful for the interpretation of D-NMR spectra from lyotropic liquid crystals. For such materials it is possible to define a principal axis system x,y,z which coincides with the symmetry axis of the lyotropic aggregates. Using this reference frame the following quantities can be defined:

$$\nu_Q^{L.C.} = e^2Q\overline{V}_{zz}/h$$

$$\eta^{L.C.} = (\overline{V}_{xx} - \overline{V}_{yy})/\overline{V}_{zz}$$

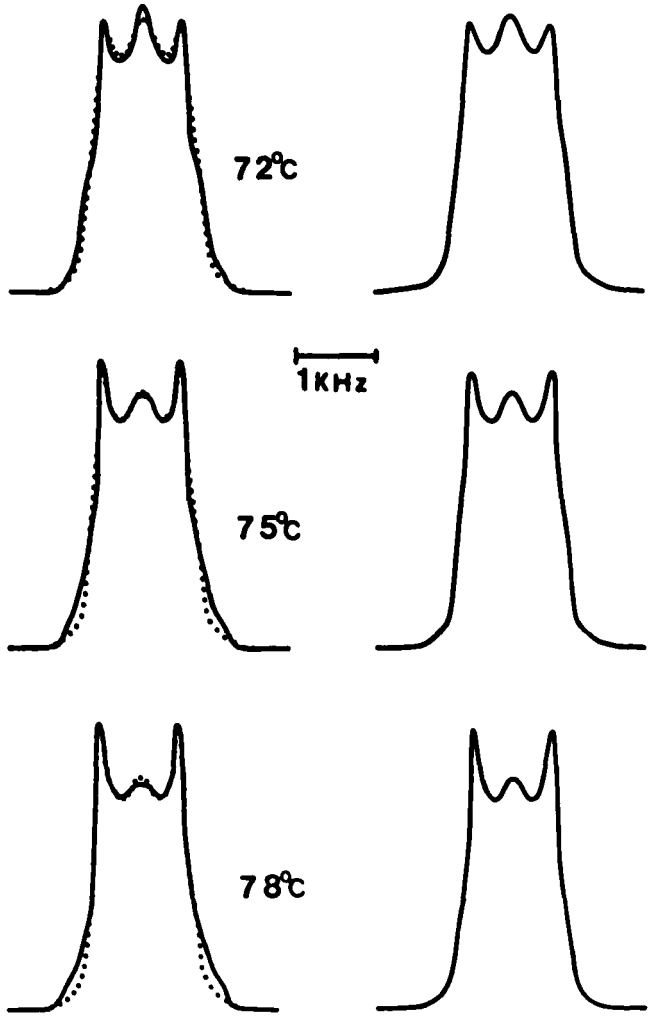

FIGURE 4 Experimental (right) and theoretical (left and dotted right for comparison) D-NMR spectral profiles of D_2O. Experimental spectra were obtained from a KP (7.92 m%)/KL (1.11 m%)/water (90.97 m% sample (sample B in Table I).

where e, Q and h are the electron charge, the quadropule moment, the Planck constant, respectively and $\overline{V}_{zz}$, $\overline{V}_{yy}$, and $\overline{V}_{xx}$ the components of the electrial field gradient tensor acting on the nucleus. These components are defined such that $|\overline{V}_{zz}| > |\overline{V}_{yy}| \geqslant |\overline{V}_{xx}|$. The geometrical factors θ_o and ϕ_o define the direction of magnetic field in the frame x,y,z. According to Abragam's theory of chemical ex-

change, the free induction decay signal can be obtained as

$$G(t) = \underset{\sim}{W}\cdot\exp\{(i\underset{\approx}{\omega} + \underset{\approx}{\pi})t\}\cdot 1 \tag{3a}$$

$\sqrt{\underset{\sim}{W}}$ being a vector which defines the probabilities of finding the molecule at the different sites. $\underset{\approx}{\omega}$ is a diagonal matrix defined such that $\omega_{\alpha\beta} = \omega_\alpha\delta_{\alpha\beta}$ · $\underset{\approx}{\pi}$ is another matrix in which elements $\pi_{ij} = \pi(\omega_i,\omega_j)$ represent the transition probability from state i to state j. One is a unit vector. The acquisition of NMR spectra by using the quadrupole echo technique requires a modification of Eq. (3a) in order to take into account that the nuclear free precession signal must be calculated after a second rf pulse, separated by an interval π, and 90° phase shifted with respect to the first 90° pulse. Since, according to Woessner,[13] the second RF pulse changes the decay $G(\tau)$, due to the first pulse, into its complex conjugate $G^*(\tau)$, Eq. (3a) can be modified as:

$$G(t) = \underset{\sim}{G}^*(\tau)\cdot\exp\{(+i\underset{\approx}{\omega} + \underset{\approx}{\pi})t\}\cdot 1 \tag{3b}$$

$\underset{\sim}{G}^*(\tau)$ being a vector defined as:

$$\underset{\sim}{G}^*(\tau) = \underset{\sim}{W}\exp\{(-i\underset{\approx}{\omega} + \underset{\approx}{\pi})\cdot\tau\} \tag{3c}$$

which represents the initial condition of the FID after the second pulse. A further modification of Eq. (3b) must be made to take into account the additional broadening process due to quadrupolar and dipolar relaxations as well as to field inhomogeneities. These effects can be introduced by multiplying Eq. (3c) by a Gaussian relaxation function.[14] Then the final equation for the FID results:

$$G(t) = \{\underset{\sim}{G}^*(\tau)\cdot\exp[(i\underset{\approx}{\omega} + \underset{\approx}{\pi})t\}\cdot 1\}R(\theta_o,t + 2\tau) \tag{3d}$$

where

$$R(\theta_o,t) = \exp[-t^2\sigma^2(\theta_o)/2] \tag{3e}$$

the width being:[15]

$$\sigma(\theta_o) = a + b(|P_2(\cos\theta_o)| - 1) \tag{3f}$$

where a and b are fitting parameters.

Before applying Eqs. 3(a–f), a certain number of assumptions need to be made. Normally when fitting the line shape obtained from lyotropic systems, the sample is assumed to be composed of domains, each corresponding to a well defined orientation. The chemical exchange of water between these domains can be neglected and the powder patterns can usually be well fitted just by considering the static overlapping of the spectra from various domains,[3] that is to say, by integration of Eq. (2) over the possible value of θ_0. Only a good approximation results, since in the time of the measurement a certain number of molecules should exchange among two or more different domains. Then, in the situation depicted in Figure 1, two different exchange phenomena should be taken into consideration when fitting the NMR powder patterns: i) exchange of water between different domains, that is, among regions characterized by a different θ_o angle; ii) exchange among different subdomains of different aggregates, in the same domain, that is, among subdomains having in common the same averaged principal axis for the quadrupolar interaction. Since normally the exchange among different domains does not seem to be a determining factor in monophase systems,[3] we did not take into account the first exchange phenomena. In applying this model, calculation of the water D-NMR powders can be done taking into consideration the exchange between two possible sites which are characterized by the two resonance frequencies:

$$\omega^{(L)} = \pm\frac{3}{4}\nu_Q^{(L)} P_2(\cos\theta_o) \tag{4a}$$

for lamellar subdomains and

$$\omega^{(R)} = \pm\frac{3}{4}\nu_Q^R\{P_2(\cos\theta_o) + \frac{1}{2}\eta^R \sin^2\theta_o \cos 2\phi_o)\} \tag{4b}$$

for ribbons subdomains.

Once the free induction signal is calculated through Eq. (3d), the FID for the powder can be obtained by integration over θ_o and ϕ_o.

It must be emphasized that if the exchange of water among differently aligned domains had been considered, a multi-site exchange model would have been necessary. In this case the problem would have been undetermined, because the number of sites corresponds to twice the number of differently aligned domains through which a molecule can travel.

Another important point is that even if one confines the possibility of exchange only among ribbons and lamellae contained in the same

domains, care must be taken in defining the principal axis systems for the two types of aggregates. It was shown elsewhere[3] that the averaged principal axis system of ribbons can coincide with that of lamellar subdomains, but the axis must be rotated by 90° when the ribbons become almost cylindrical.

Numerical calculations of theoretical powder patterns were done by using a modified version of the program EXCHANGE.[16] The input parameters were: i) the population ratio of the two sites $WR = W^{(L)}/W^{(R)}$; ii) the frequency of jumping between the two sites, K, which is the only independent element of the matrix $\overline{\overline{\pi}}$; iii) the quadrupolar couplings in the lamellar and ribbon mesophases $\nu_Q^{(L)}$ and $\nu_Q^{(R)}$, respectively; and iv) the asymmetry parameter of the ribbon mesophase η^R. The broadening parameters (a) and (b) in Eq. (3f) have been assumed to be 50 Hz and 150 Hz which are reasonable values usually employed to fit spectra in the L_α mesophase where the spectral singularities are much sharper than in the spectra reported in Figure 4.

The theoretical spectra in Figure 4 were calculated by using $\nu_Q^{(L)} = 1$ KHz, $\omega_Q^{(R)} = 0.78$ KHz and $\eta = 0.83$. These values and the line broadening parameters of Eq. (3f) were obtained from spectral patterns recorded in the lamellar and ribbon phases. The only fitting parameters used for the spectra of Figure 4 were $K = 200$ kHz and the population ratio WR. The best values were $WR(72°C) = 0.7 \pm 0.1$, $WR(75°C) = 1 \pm 0.1$, $WR(78°C) = 1.4. \pm 0.1$. The value of K (200 kHz) is responsible for rounding off the peaks of the patterns and we believe that it is a very crude value which only gives a rough idea of the physics of the system because of the restrictive assumptions included in the calculation. Nevertheless this method can be used to obtain valuable information which cannot be obtained by other techniques. If the mean value of 1.5×10^{-5} cm²/sec is taken for the diffusion coefficient of the water in the temperature range between 72° and 78°C (see Figure 3), and defining the time $t = 1/K$ as the averaged interval of time that a molecule spends in each subdomain, then the mean dimension of subdomains d can be calculated according to the relation $d = \sqrt{2Dt}$. The resulting value of $d = 4\mu$ is probably a value not far from reality, despite the rough model employed.

In conclusion, diffusion measurements and line shape analysis of D_2O spectral profiles in KP/KL/water lyotropic mixtures confirm the previously reported interpretation of the occurring mesophases. Further, the experimental data allowed deriving a valuable even if quite rough structural parameter concerning the spatial distribution of the lyotropic aggregates.

Acknowledgment

The authors acknowledge Mr. D. DeFazio for taking some of the PFG measurements, Mr. L. Covello for technical assistance, and the Italian Ministry of Education (M.P.I) for financial support. One author (JWD) acknowledges NSF support under Solid State Chemistry DMR82-44468.

References

1. P. Ekwall, in "*Advances in Liquid Crystals*," Vol. 1, Ed. G. H. Brown (Academic Press, New York, 1975), pp. 1–139.
2. S. Benigni, Ph.D. Dissertation, Kent State University, 1982; S. Benigni, G. Chidichimo, Z. Yaniv, J. W. Doane and N. Spielberg, 9th International Liquid Crystal Conference, Bangalore, India, December 1982.
3. G. Chidichimo, N.A.P. Vaz, Z. Yaniv and J. W. Doane, *Phys. Rev. Lett.*, **49**, 1950 (1982).
4. G. Chidichimo, A. Golemme and J. W. Doane, *Bull. of Mag. Res.*, **5**(314), 137 (1983).
5. R. Blinc, K. Easwaran, J. Pirs, M. Volfan and I. Zupančič, *Phys. Rev. Lett.*, **25**, 1327 (1970).
6. G. Chidichimo, A. Golemme and J. W. Doane, *J. Chem. Phys*, **82**, (April 1985).
7. G. Chidichimo, A. Golemme, P. Westerman and J. W. Doane, *J. Chem. Phys.*, **82**, 536 (1985).
8. E. D. Stejskal and J. E. Tanner, *J. Chem. Phys.*, **42**, 288 (1965).
9. D. I. Hoult and R. F. Richards, *Proc. Roy. Soc., London Ser. A*, **344**, 311 (1975).
10. G. A. Ranieri, et al. (unpublished results).
11. A. Abragam, "*The Principle of Nuclear Magnetism*" (Oxford Unviversity Press, London, 1962).
12. D. J. Photinos, P. J. Bos, M. E. Neubert and J. W. Doane, *Phys. Rev. A*, **20**, 2703 (1979).
13. D. E. Woessner, B. S. Snowden and G. M. Meyer, *J. Colloid Interface Sci.*, **34**, 43 (1970).
14. J. H. Davis, K. R. Jeffrey, M. Bloom, M. I. Valic and T. P. Higgs, *Chem. Phys. Lett.*, **42**, 390 (1976).
15. D. J. Photinos, P. J. Bos, J. W. Doane and M. E. Neubert, *Phys. Rev. A*, **20**, 2203 (1979).
16. M. A. Rance, Ph.D. Dissertation, University of Guelph, 1981.